Polymer Micromixers Bonded to Thermoplastic Films Combining Soft-Lithography with Plasma and APTES Treatment Processes

Michael Lee,[1] Maria J. Lopez-Martinez,[2†] Abdellatif Baraket,[1] Nadia Zine,[1] Jaume Esteve,[2] Jose A. Plaza,[2] Nicole Jaffrezic-Renault,[1] Abdelhamid Errachid[1]

[1]Université de Lyon, Lyon1, Institut des Sciences Analytiques (ISA), UMR 5280, 5 Rue de la Doua, 69100 Villeurbanne Cedex, France
[2]Instituto de Microelectronica de Barcelona, IMB-CNM (CSIC) Campus UAB, 08193, Bellaterra, Barcelona, Spain
Correspondence to: M. Lee (E-mail: michael.lee@etu.univ-lyon1.fr) or A. Errachid (E-mail: abdelhamid.errachid@univ-lyon1.fr)

Received 1 June 2012; accepted 11 September 2012; published online 9 October 2012
DOI: 10.1002/pola.26387

ABSTRACT: Over the past few years, a growing interest on covalent bonding of polydimethylsiloxane (PDMS) microfluidic devices to thermoplastic films has developed due to reduced costs, biocompatibility, and flexibility. The silane reagent, 3-aminopropyltriethoxysilane (APTES) has been applied to create this bonding. Here, we report on the fabrication of replica PDMS micromixer devices from a silicon mold using soft lithography that is rapid, facile, and cost-effective to manufacture. After replica molding, the PDMS micromixer devices were bonded to the APTES-activated thermoplastic films of polyimide, polyethylene terephthalate, and polyethylene naphthalate. Characterization of these thermoplastic surfaces was analyzed by contact angle measurement, surface free energy, and X-ray photoelectron spectroscopy. To demonstrate the functionality of this technology, we have analyzed the PDMS micromixers by a peel test, nonleakages, and mixing with the injection of inks, a surfactant, and varying pH solutions. To our knowledge, this is the first reported example in literature of the PDMS–APTES–thermoplastic films preparation that integrates a complex micromixer device. Here, we have established that the hydrophobicity of both sealed polymers required alteration in order for dispersion of a polar liquid in the mixing loops. The application of a polar solvent before injection can remedy this ill effect formulating a hydrophilic micromixer. These preliminary results demonstrate the feasibility of the fabrication technology, bonding technique, and application of the micromixer that, once optimized, can eventually integrate more components to formulate a lab-on-a-chip with the fabrication of gold microelectrodes for biological analysis of blood or plasma. © 2012 Wiley Periodicals, Inc. J Polym Sci Part A: Polym Chem 51: 59–70, 2013

KEYWORDS: APTES; functionalization of polymers; micromixer; mixing; thermoplastics

INTRODUCTION In the past decade, the field of microfluidics has evolved and expanded by the application of various materials.[1,2] In this time, the simple fabrication and implementation of polydimethylsiloxane (PDMS) microfluidic devices has been restricted to silicon and glass-based substrates.[3–5] For optical detection, silicon is not optically transparent in the desired wavelength, though it is structurally strong. Glass has outstanding optical properties throughout the visible spectrum, and is highly resistant to solvents.[6] Unfortunately, when compared with silicon, glass is fragile. Therefore, thermoplastic films have become more compelling as an increase in literature has proven that these films can be enclosed with PDMS microfluidic devices.[7,8] The versatility and expense when compared with silicon or glass-based substrates has helped create reduced costs on a larger production scale as they can be easily mass produced.[9] Importantly, due to the varying surface environments of different films (surface, optical, and mechanical properties), then these films can be chosen for a specific application that can be influenced to the largest extent.[10] Therefore, these thermoplastic films are advantageous due to their biocompatibility, flexibility, and improved disposability. In this instance, the cost-effectiveness of applying PDMS with bonded thermoplastic films comes into prominence when designing and fabricating a lab-on-a-chip. The incorporation of a PDMS microfluidic device (mixers, filters, etc.) with microelectromechanical systems based on thermoplastic films reduces cost, fabrication time, and the requirement of expensive laboratory equipment for microelectrode fabrication on silicon or glass (e.g., photolithography) that requires cleanroom conditions. By application of thermoplastic films, gold microelectrodes can be developed rapidly by microcontact printing or electroless deposition using a structured PDMS mold after the initial fabrication and soft lithography of a silicon master.[11] In all these can outweigh the advantages when

†*Present address:* The University of Hull, Department of Chemistry, Cottingham Road, Hull, HU6 7RX, United Kingdom.

applying silicon or glass-based substrates. However, unlike silicon or glass substrates, irreversible bonds between PDMS and thermoplastic films cannot be formulated directly with oxygen plasma.[12] Here, bonding can occur, however, on injection or washing with water, the bonds are broken by hydrolysis. Therefore, the application of 3-aminopropyltriethoxysilane (APTES) will create the necessary chemical bonds that formulate a highly polar surface and an increased surface free energy (SFE).[13] Surface modification by oxygen plasma followed by incubation with APTES will formulate triethoxysilane groups ($Si(OEt)_3$) on the thermoplastic films surface. This technique is rapid (20-min incubation) and, therefore, does not present an undesirable increase in activation time when compared with the solitary oxygen activation of silicon or glass. Generally, APTES is dissolved in a polar solution, for example, water or ethanol, as this will elevate the hydrolyzation of $Si(OEt)_3$ groups to silanol groups ($Si(OH)_3$). Essentially, this produces a chemical composition that is similar to oxygen-activated glass, which enables PDMS–thermoplastic film microfluidic devices to be enclosed. It must be noted that as the repeating unit for the chemical structure of glass is Si—O—Si, and with the oxygen activation of PDMS being similar, the bonding of the two produces strong Si—O—Si bonding. For thermoplastics films, the repeating unit contains varying functional groups. Here, the repeating chains are made up of some carbonyl groups that are activated to have affinity to the amine functionality of APTES. The silanol groups that are hydrolyzed at the other end of the hydrocarbon chain formulate the chemical composition similar to glass.

Recently published articles have applied APTES as a chemical reagent for PDMS–thermoplastic film bonding.[14–17] For instance, Aran et al. have applied nanoporous polycarbonate, polyethersulfone, and polyester terephthalate.[15] These porous polymer membranes were treated with APTES (5% v/v in water) and bonded with two PDMS layers for a microfiltration microdevice. Also, Tang et al. have applied poly(methylmethacrylate) (PMMA), polycarbonate (PC), polyimide (PI), and polyethylene terephthalate (PET).[16] An aqueous solution of APTES (1% v/v) was applied for PDMS bonding of a serpentine microchannel (186 mm $\times$ 500 μm $\times$ 150 μm). Finally, Sunkara et al. have treated PC, cyclic olefin copolymer, PMMA, and polystyrene (PS) with APTES (1% v/v in an aqueous solution).[17] Here, large-sized PDMS microchannels were applied for leakage tests (70 mm $\times$ 800 μm $\times$ 45 μm). In these articles,[16,17] the authors have studied and provided a great deal of information on bond strength for an ink moving in a one-directional microchannel. In microfluidics, a micromixer is an essential device that is applied for rapid mixing, and by bonding the PDMS micromixers with PI, PET, and polyethylene naphthalate (PEN), the physical and mechanical properties will change. The hydrophobic properties of the PDMS–APTES–thermoplastic films can prevent the fluid from flowing into the mixing loops, because injection of a polar liquid will prevent dispersion of the liquid as cohesive forces are more predominant. This effect is unseen if microchannels have only one fluidic flow route, because dispersion is not a requirement from liquid input to output.

Micromixing systems that consist of active mixing components have for instance used electrokinetics, pressure disturbances, electrohydrodynamics, magnetohydrodynamics, and acoustics.[18] These systems rapidly formulate an increase in the mixing process due to the external disturbance that has been generated. However, although active mixers can have excellent mixing capabilities, active micromixers are difficult to integrate with other microfluidic components and due to their relatively high costs, they are not beneficial to be applied as a disposable device.[19] On the other hand, passive micromixers have lower costs, easier to fabricate, and can be integrated into microfluidic systems or micro-total analysis systems (μ-TAS). As there are no moving parts or the requirement of power and control, these devices are more reliable for mixing.[19] In a review of micromixer designs, passive micromixers with chaotic advection commonly generate the mixing process within the microchannel itself due to the designed geometries. These micromixers with chaotic advection have included Tesla structures, C-shape, L-shape, and twisted microchannels, and so forth that are based on 2D or 3D geometries.[20–22] The modification of the flow pattern due to the random manner that a fluid will cross the flow path within the microchannel with small volumes traveling at small distances is vastly increased, and this leads to rapid and continuous mixing.[23,24] Theoretically, for passive micromixers without chaotic advection a microfluidic device relies only on molecular diffusion within Y-shaped or T-shaped configurations.[25] These require long microchannels in order of ensuring that diffusion has occurred though these are inefficient and time consuming.[26] The efficiency of micromixing is determined by the interfacial area of where the two liquids mix as a cause of molecular diffusion and chaotic advection. The greater the area, the greater the mixing will be. At the microscale, diffusion is rapid and the flows are laminar.[27] Because of the topology, passive mixers enable the two liquids to mix subsequently. Here, we have designed a mixing geometry on the microscale that has a short microchannel, although it is efficient at micromixing due to 18 external mixing loops with reduced mixing loop dimensions to formulate fluidic propulsion at the point of the mixing loop exits. These mixing loops create the required force that enables the two liquids to cross streams and, therefore, continuously circulate and mix within the microchannel. By this modification in the design, the laminar flow within the microchannel can be manipulated to produce chaotic advection.

The proposed micromixer device consists of a thin PDMS replica ($\sim$1.75 mm) with a total surface area of 6 $\times$ 4 mm^2 in length/width, respectively. These dimensions can play a pivotal role in preventing adequate bonding because a smaller surface area (24 mm^2) was applied, and therefore, applied pressure was necessary to ensure conformal contact. For the micromixer geometries, the dimensions were dramatically reduced again in comparison to the aforementioned articles with 15 -μm-width mixing loop exit and a height of $\sim$71 μm. The dimensions of the microchannel were $\sim$6.2 mm $\times$ 100 μm $\times$ 71 μm. Once the system was enclosed, two different dyes were used for the evaluation of mixing. To our

knowledge, we have exhibited the first complex PDMS micromixing device, chemically bonded onto the aforesaid thermoplastic films, and by injection of two dyes, we have demonstrated the first results of micromixing on two hydrophobic materials. An emphasis of mixing has been studied by injection of a surfactant, and the mixing performance based on pH measurements is also shown to demonstrate the novelty and advantage of the mixing geometry. These devices will essentially analyze biological material, where incorporation of microfilters can aid in sample preparation, separation, and detection of the required response. By analyzing the effects of water-based solutions within the micromixer using two dyes diluted with water, we can evaluate the approach when analyzing polar-based solutions where fluidic dispersion is a requirement.

MATERIALS AND METHODS

Materials and Techniques

Polymers

The applied thermoplastic films were PI (HN 125 μm DuPont), PET (200 μm Goodfellow), and PEN (160 μm Goodfellow). PDMS (Sylgard 184) was purchased from Dow Corning, France.

Chemicals and Reagents

All chemicals were purchased from Sigma-Aldrich, France, except toluidine blue, which was obtained from Carl Roth, France, and iron(III) nitrate nonahydrate from Acros Organics, France.

Optical Imaging

All optical microscope images were made with an Olympus BX41M (France) and Leica Microscope EZ4D (Spain). Finally, scanning electron microscope (SEM) images were obtained with a SEM 515 Philips, The Netherlands.

Contact Angle Measurement

The surface of the three polymer films (PI, PET, and PEN) were characterized by contact angle measurement (CAM; GBX Scientific Instruments, France). The cleaned polymers, oxygen activated, and APTES functionalized, were analyzed by advancing contact angle using deionized water. Propanol was also analyzed for determining the hydrophilicity on the cleaned polymer surfaces.

Surface Free Energy

By the Owens and Wendt Model, the polar and dispersive components of the polymer films surface energy were calculated. Here, cleaned polymers and polymers activated with APTES (6%) were analyzed. PDMS and glass activated by oxygen plasma provided results for comparison. Here, the water droplet was dispensed by a mechanical syringe that was operated manually. All measurements were made by depositing 1 μL of each liquid (deionized water, diiodomethane, and formamide) at 24 °C $\pm$ 2. Six values were recorded for all liquids on each polymer. The precision of the microregulator was 0.33 μL for a 1 -μL drop. The results for CAM and SFE were recorded by the Windrop++ software.

X-Ray Photoelectron Spectroscopy Analysis

X-ray photoelectron spectroscopy (XPS; Instruments PHI Quantera SXM) established the elemental analysis of silanol-based groups with a depth analysis of $\sim$3 nm. The aluminum X-ray radiation source was 1486.6 eV, with a pressure chamber of 3×10^{-9} Torr. The voltage and current of the anode were 15 kV and 3.3 mA, respectively. The take-off angle was positioned at 45°. The threshold of atomic detection was between 0.1 and 0.5%, and a precision of 2–5%.

Aspects of the Micromixing Device

The design and fabrication process of the silicon micromixer were fabricated simultaneously with microdispensers already published.[28,29] The novelty of the micromixer consists of the versatility of the micromixer fabrication technology. Here, the silicon chip has been bulk-micromachined by deep reactive ion etching (DRIE). DRIE provides excellent aspect ratios, and the technique can mill deep trenches with large lateral accuracy.[30] This has defined very precise cavities and, thus, avoided unfavorable connecting paths among the microchannels.[28] For the designed micromixer, the incorporation of 18 mixing loops enables complete mixing to occur within the microchannel. As passive mixers are known to require long microchannels for molecular diffusion to occur, here, the advantage of the mixing geometry enabled the fabrication of a shortened microchannel length. This was due to the recirculation of the fluids that was created by the mixing loops. The geometry of the mixing loops increase the velocity within the microchannel. As a direct cause to this phenomenon, the two injected samples completely mix. In reference to the designed mixing geometry, the advantage of the fabrication process does not require complicated masks. For instance, C-shape, L-shape, and twisted channels integrate complex and fine 3D designs to create chaotic advection with intermediate Reynolds numbers. The fabrication of these designs is time consuming and is more intricate to manufacture. For the versatility of the applied technology, the design process using the required masks can easily incorporate a variety of additional active microfluidic components (e.g., microfilters). These can be implemented as a photolithographic step and, therefore, avoid any additional fabrication step requirements.[28] Therefore, this can provide a microtechnology platform that is cost-effective and efficient for producing micromixers capable of creating complete mixing without the requirement of 3D or complex structure integration.

The two injection ports for the simultaneous introduction of two liquids have been specifically designed for mixing [Fig. 1(a)]. Once the two liquids are injected, they flow through the Y-inlet with a width of 200 μm. On entering the main microchannel, the width is reduced to 100 μm. This decreases the diffusion path of the two liquids as they flow parallel to one another. Then, the liquids enter the first 50-μm-width mixing loop. The decrease in width increases the velocity of the liquid. The exit of the loop is reduced to a width of 15 μm [Fig. 1(a′)] so that the liquids are propelled back into the microchannel producing increased chaotic fluidic flow to enhance the mixing efficiency. The liquids return to the wider microchannel where they encounter the next micromixing loop to increase mixing. In total, there were 18 external micromixing loops along the microchannel. The total length of the microchannel has a decreased length of 6.2 mm, and with 18 mixing loop geometries, a high-throughput of mixing can be created to ensure that the two injected samples have been comprehensively and continuously mixed.

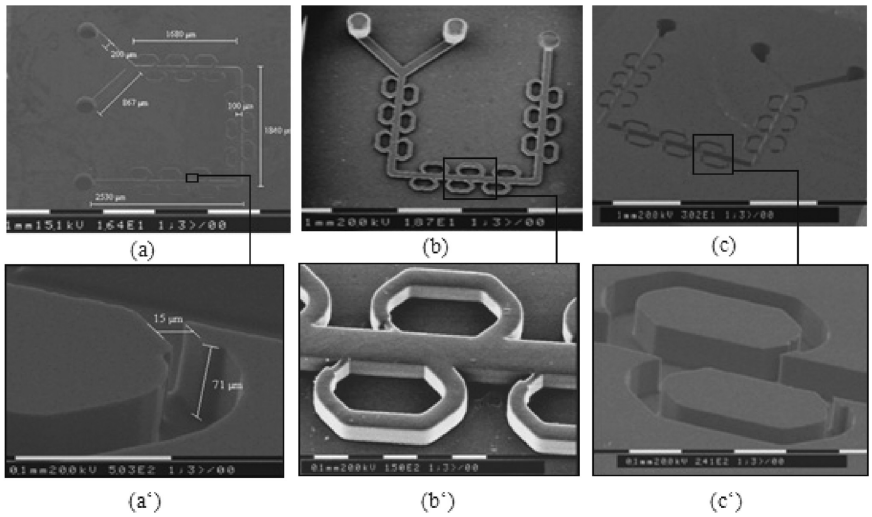

FIGURE 1 SEM images of micromixer fabrication, where (a) micromixer manufactured into silicon wafers, (b) first PDMS replica mold at a mixing ratio of 5:1 producing positive micromixer features, and (c) the final PDMS micromixer at the standard 10:1 mixing ratio.

Fabrication Technology

Replica Molding from Silicon to PDMS

After the fabrication of the silicon micromixer, the structured silicon substrate was cleaned and the surface was then silanized.[31] The silicon micromixer mold consisted of an etched microfluidic channel with positive features, and therefore by soft lithography, two PDMS molds were required to form an exact replica. From the silicon-based mold, a positive elastomeric replica was fabricated. Here, a 5:1 PDMS ratio of the elastomer:crosslinking agent (w/w) [Fig. 1(b)] was poured on-top of the silicon mold, and the mixture was cured at 90° for 1 h. The silicon master was removed from the PDMS, and this left a cavity in the PDMS that was used for the next replication process.

After the fabrication of the first PDMS replica, the mold was then coated with gold (~6.25 nm) using an Emscope SB 500 Sputter Coater (France) for 30s (−1 Torr). The deposition of a thin layer of gold acts as an antiadhesive layer that ensures the positive and negative PDMS replicas will separate after curing.[32] Finally, a standard 10:1 PDMS mixture (w/w) was poured into the cavity of the first PDMS replica to produce the final mold. The second mold was also cured at 90° for 1 h [Fig. 1(c)]. The variation between the PDMS ratios ensured well-defined structures had formed from the first mold (decreased elasticity) to facile demolding with the second PDMS mold, because the Young's modulus was varied. The fabrication of the second mold produced an exact replica of the original silicon master. This demonstrated the feasibility of double replication in PDMS from a single silicon master.

Activation Process

Thermoplastic Film Treatment with APTES

The polymer substrates PI, PET, and PEN were cleaned by sonication in propanol, followed by Milli-Q water for 10 min. The substrates were rinsed in Milli-Q and dried with nitrogen. Afterward, the thermoplastic films were treated with oxygen plasma (Plasma Technology) for 1 min (90 W, 100 mTorr), and placed directly in an aqueous solution of APTES (6% v/v) for 20 min at 90 °C. Finally, the substrates were rinsed in Milli-Q and dried with nitrogen.

Plasma Treatment of PDMS Micromixers and Adhesion

The second PDMS replicas were cleaned by sonication in ethanol for 10 min, followed by rinsing in Milli-Q, and dried with nitrogen. The PDMS were allowed to stand for 10 min to ensure of deswelling. The PDMS replicas were activated by oxygen plasma for 20 s (90 W, 100 mTorr). After this activation period, the PDMS replicas were placed in direct contact with the APTES-modified thermoplastic films (PI, PET, and PEN). To ensure that conformal contact was made, slight pressure was applied between the PDMS and the polymer films. However, an increased amount of pressure was eventually required to prevent fluidic leakage. The enclosed micromixers were left at room temperature for 1 h. This ensured that irreversible bonding between the two polymers had interacted and strengthened by Si—O—Si bonding at the PDMS–thermoplastic film interface.

Application: Micromixing

Nonleakage Tests and Injection of Two Dyes

After the bonding process between the PDMS micromixers to the thermoplastic films, nonleakage tests were carried out. Initially, toluidine blue was injected through one of the inlet ports, and the flow inside the channel was followed by an optical microscope.

To ensure simultaneous injection, the introduction of the two dyes (toluidine blue and iron(III) nitrate nonahydrate) into the microchannel consisted of back aspiration through the exit port. Here, manual injection was made with two syringes containing the different inks. These were connected to the injection ports. A third syringe was connected to the exit port to aspirate manually the two inks and to make them enter the microchannel simultaneously.

Injection of a Surfactant

The injection of the surfactant and toluidine blue were carried out as previously mentioned in Nonleakage Tests and Injection

TABLE 1 Advanced Contact Angles Using Deionized Water of Cleaned PI, PET, and PEN Films Followed by Oxygen Plasma Oxidation and APTES Incubation

	PI	PET	PEN	PDMS	Glass
Cleaned substrates	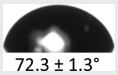 72.3 ± 1.3°	 73.7 ± 2.5°	 81.7 ± 1.2°	 107.4 ± 1.1°	–
1. Oxygen activated	8.7 ± 0.4°	8.5 ± 1.0°	7.0 ± 0.6°	6.3 ± 1.8°	4.5 ± 0.3°
2. APTES (6%) in water	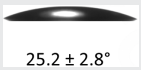 25.2 ± 2.8°	 38.8 ± 1.1°	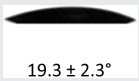 19.3 ± 2.3°	–	–

of Two Dyes section. The aim of this analysis was to observe the velocity of propulsion created by the mixing loops. The formation of globules or air bubbles as an effect of the varying dimensions can demonstrate the functionality of the micromixer. In this instance, to observe mixing with the two varying colors and with the creation of air bubbles, therefore, specifies the mixing geometry is capable of creating mixing due to the developed mixing loops within the microfluidic device.

Mixing Performance by pH Measurements

The injection of two varying pHs were carried out as previously mentioned in Nonleakage Tests and Injection of Two Dyes section. To demonstrate the mixing performance of the micromixer device a pH analysis was analyzed. Here, a solution of Tris(hydroxymethyl)aminomethane (TRIS 99+%, pH 9 at 1 *M*) with the pH varied accordingly by potassium hydroxide (KOH at 1 *M*) and hydrochloric acid (HCl at 1 *M*) to formulate pH 10 and pH 2, respectively. A control was prepared by analyzing the solutions (pH 10 and pH2) directly with litmus paper. This was followed by mixing equal quantities of the two solutions by vortex. The resulting solution was transferred to litmus paper to formulate the new pH reading. For the micromixer, the outcome of the two injected pHs were analyzed by litmus paper at the exit port to observe whether complete mixing could be achievable with the designed geometry of the micromixer.

RESULTS AND DISCUSSION

Surface Characterization

Contact Angle Analysis

To demonstrate the feasibility of PDMS–APTES–thermoplastic films bonding, characterization was made by CAM to determine wettability and SFE requirements. Treatment with oxygen plasma revealed a substantial increase on the hydrophilicity of the polymer films (PI, 9°; PET, 9°; and PEN, 7°) and PDMS (6°) (Table 1). The oxidation process facilitated the chemical functionalization with APTES. After the incubation with APTES/water, the wettability on all three thermoplastic films was still abundantly hydrophilic at PI, 25°; PET, 39°; and PEN, 19°. This confirmed the chemical modification of the thermoplastic films.

As the preferential choice of PDMS microfluidics has been bonded to glass, we have observed the required surface energy that permits these devices to be enclosed. By the Owens and Wendt Model, applying a three liquid analysis, the oxidation of glass generated a SFE total of 72 mN/m and oxidized PDMS was 71 mN/m (Table 2). Through the activation of repeating —Si—O—Si— bonds, the polar composition taken against the energy total of both materials was calculated at ~50%. The SFE on the thermoplastic films provided increased energy totals when compared with nonfunctionalized films. Here, the calculated energy totals were close to the value obtained for glass (PI, 68 mN/m; PET, 64 mN/m; and PEN, 70 mN/m). Therefore, the polar composition also showed a definitive increase (PI, 40%; PET, 33%; and PEN, 45%).

Here, the values demonstrate that APTES has activated the polymer films surface and that the polymer films surface can reproduce an energy total similar to that of oxygenated glass. Thus, the chemical functionalization with APTES on thermoplastic films can be replicated in a similar fashion to the activation of glass.

TABLE 2 SFE of Cleaned Polymers and Activated in APTES/Water with Clean and Oxygen-Activated PDMS

	PI		PET		PEN		PDMS		Glass
	Clean	APTES	Clean	APTES	Clean	APTES	Clean	O_2	O_2
Energy total	48.1	67.7	44.8	64.2	42.0	69.7	19.1	71.4	72.1
Polar composition	5.6	27.3	5.0	21.1	2.7	31.0	0.2	36.8	34.9
Dispersive	42.5	40.4	39.8	43.1	39.3	38.7	19.0	34.6	37.2
Polarity (%)	11.6	40.3	11.2	32.9	6.4	44.5	1.0	51.5	48.4

Oxygen-activated glass demonstrates the required SFE required for the polymer films to bond to activated PDMS (Values in mN/m).

TABLE 3 The Atomic Percentages of Cleaned Polymer Substrates with APTES-Activated Polymers

Atomic %	C	O	Si	N	O/C	N/C	N/Si
PI–ref	76.3	16.9	–	6.8	0.22	0.09	–
PI–APTES	53.9	29.6	5.3	9.9	0.55	0.18	1.9
PET–ref	71.5	28.5	–	–	0.40	–	–
PET–APTES	66.5	27.9	2.4	2.8	0.42	0.04	1.2
PEN–ref	77.5	21.9	0.6	–	0.28	–	–
PEN–APTES	62.0	28.4	2.7	3.0	0.46	0.05	1.1

XPS Analysis

To demonstrate the elemental composition of functional $Si(OH)_3$ groups on the thermoplastic films, characterization was made by XPS. On APTES-activated PI, PET, and PEN films the atomic percentage of carbon, C (%) was reduced (Table 3). This signifies that the nonfunctionalized polymers have been chemically modified through the repeating hydrocarbon chains. For O (%), PI-modified and PEN-modified films detected an increase when compared with bare films, whereas PET/APTES decreased. The increase in O (%) related to an increase in polarity on the surface, that is, the functionalization with $Si(OH)_3$. The decrease in O (%) on PET/APTES can relate to CAM results where water angles and SFE were lower than expected. The presence of $Si(OH)_3$ was confirmed by silicon, Si (%) on all three polymers. On the bare polymers, no Si was detected (small contamination on PEN at 0.6%). Following APTES incubation, the polymers contained Si at PI, 5.3%; PET, 2.4%; and PEN, 2.7%. This result was verified by the content of nitrogen, N (%) as the amino properties in APTES. Here, an increase in N (%) was observed with PI, 3.1%; PET, 2.8%; and PEN, 3.0%. Though contaminants were detected there was no form of degradation to the $Si(OH)_3$ groups. As a result, the XPS analysis verified that PI, PET, and PEN were effectively activated with APTES to formulate $Si(OH)_3$ groups.

Fabrication Technology and Bonding Tests

Peel Test

To ensure achievable PDMS–APTES thermoplastic film bonding, a peel test was applied by pulling the two substrates apart. In Figure 2, the Si—O—Si bond formation was observed, and a high bonding strength was observed. Here, the PDMS was removed from the PI, PET, and PEN films, with ripping occurring within the PDMS matrix. This signifies that the PDMS–APTES thermoplastic film interface was integral and fundamental to the covalent bonding of functional $Si(OH)_3$ groups on the activated thermoplastic films surface.

Replica Molding

After ensuring that the PDMS could bond to the varying thermoplastic films, the PDMS micromixers were bonded to the PI, PET, and PEN films. A cross section of a PDMS device bonded to PI is shown in Figure 3 by SEM. Six square holes in Figure 3(a) consisted of two microchannels and either side of this were two mixing loops, respectively. The total thickness of the microdevice was $\sim$1.75 mm, whereas the dimensions of the fully reproduced PDMS device were 6×4 mm^2 in length/width, respectively. Here, the dimensions of the PDMS devices were relatively small (surface area of 24 mm^2), and as the topography of the PDMS surface is not homogenous, a small amount of applied pressure was applied. This was to induce conformal contact of the PDMS device with the polymer film. At this stage, it was perceived that too much pressure could cause deformation of the structures (e.g., 15-μm-width mixing loop exit) within the PDMS micromixer, and therefore, a minimal pressure approach was implemented here.

The height of the microchannel was $\sim$71 μm, and this produced a low aspect ratio, which was adequate for bonding. The image [Fig. 3(b)] shows a magnified region of the microchannel, where the mixing loops exit is clearly observed.

Nonleakage Tests—Injection of Toluidine Blue

The optical image in Figure 4(a) shows a PDMS micromixer bonded to PI. The device showed good adhesion because no leakage was visible within the system; however, the dye was incapable of entering into the mixing loops. For PDMS bonded to PET [Fig. 4(b)], the dye entered into some of the mixing loops but not all, whereas some leakage of the dye was seen diffusing from the corners of the mixing loops. Here, the slight pressure approach was applied. Finally, PDMS bonded to PEN [Fig. 4(c)] showed adhesion between both polymer layers. A similar problem was evident with the ink being unable to enter into the mixing loops.

At first, it was perceived that the ink was unable to flow into the loops because of a possible collapse within the mixing loops. The mixing loop exit has a width of 15 μm and a depth

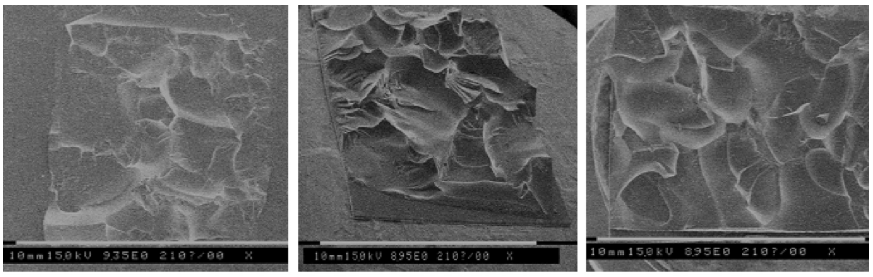

FIGURE 2 SEM images of a peel test demonstrating bonding strength on (a) PI, (b) PET, and (c) PEN.

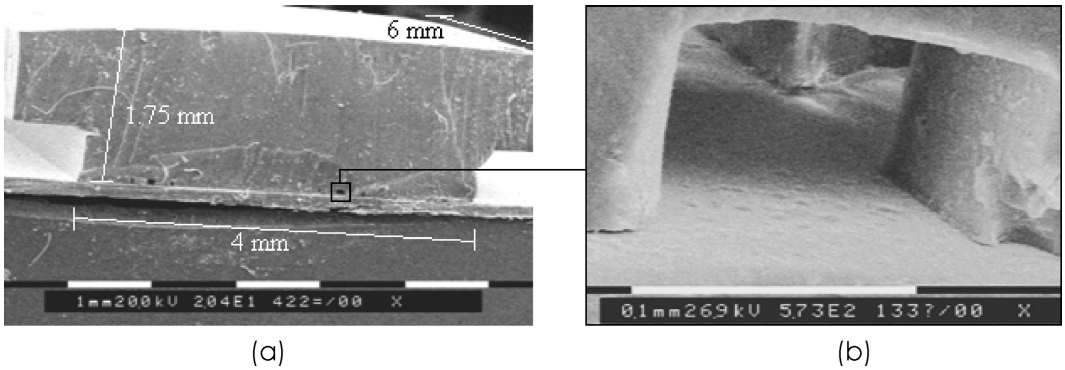

FIGURE 3 SEM images of a PDMS micromixer device bonded to PI film showing a cross section of (a) the overall dimensions of the device (6 × 4 × 1.75 mm) with two visible microchannels and (b) magnified view of a microchannel with mixing loop exit.

of 71 μm. This aspect ratio falls within the standard 10:1 range. The phenomenon of gravity upon the elastomeric features can cause an affect known as "buckling" or "pairing." This is where large aspect ratios (height > width) collapse under their own weight due to the application of force.[33] In this instance, it was supposed that the micromixer aspect ratios were unstable and unable to support themselves upon adhesion to the polymer film. Therefore, the slight pressure approach was applied for bonding the PDMS–thermoplastic film. However, the cross section [Fig. 3(b)] exemplified that this was not the case since the mixing loop exit was clearly open. This was also supported by injection of toluidine blue into a PDMS micromixer based on glass. Here, the ink flowed into all mixing loops [Fig. 4(d)]. The theoretical collapse of the height being greater than the width causing pairing was not the cause of the ink being unable to disperse into the mixing loops. The phenomenon was accountable to the hydrophobic nature of both the PDMS micromixer and the thermoplastic films. As a result, all resulting bonding processes were made with increased pressure to ensure homogenous conformal contact of the PDMS–thermoplastic film preparation.

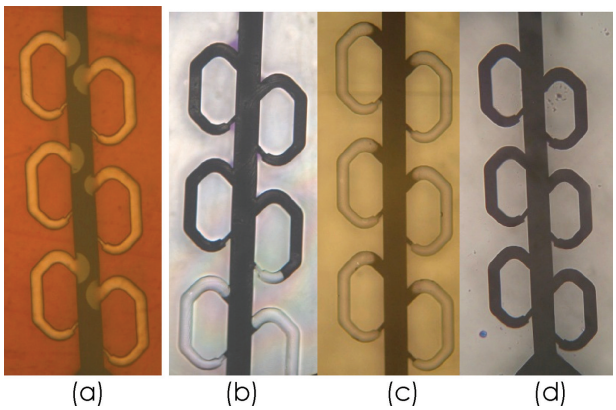

FIGURE 4 A section of the PDMS micromixers by optical microscopy showing toluidine blue injection on (a) PI, (b) PET, (c) PEN, and (d) glass. Here, slight pressure was applied for the PDMS–thermoplastic bonding.

Polymer Hydrophobicity Alteration

The introduction of propanol, followed by the injection of toluidine blue has enabled the ink to travel into all the mixing loops. The analysis of contact angles by applying propanol on the three nonactivated polymer substrates was observed (Table 4). Previously, the results have shown that all bare polymers (PI, 72°; PET, 74°; and PEN, 82°) were less hydrophilic when analyzed with deionized water (Table 1). By analyzing the angles on the same polymers with propanol, the films became highly hydrophilic (PI, 6°; PET, 5°; and PEN, 7°). This highly hydrophilic nature of propanol enabled the solvent to travel through the entire micromixer. A water-based solution such as toluidine blue could not enter into these mixing loops due the hydrophobic nature of the polymers. This caused an increase in the cohesive forces that only permitted the polar liquid to travel around the microfluidic channel rather than flowing into the mixing loops. Therefore, the fluidic flow of polar liquids in PDMS/glass is due to the hydrophilic nature of glass.

In Figure 5(a), toluidine blue injection into the microdevice based on PET shows prior propanol injection. Propanol has increased the hydrophilic nature of the polymer surface, and in comparison to Figure 4(b), there is an improvement of the ink entering into the mixing loops (some loops do not function and they appear to have been malformed during the replication process). With applied pressure to an area near the mixing loops [Fig. 5(b)], the PDMS device has been deformed. After applied pressure, the microdevice regained its original shape with no leakage visualized due to the elasticity of PDMS [Fig. 5(c)]. Here, an increased an amount of pressure was applied during the bonding process as structural collapse was not the issue. This has improved bonding

TABLE 4 Advanced Contact Angles of Cleaned PI, PET, and PEN Films Using Propanol for Analyzing the Wettability of the Polymer Films

PI	PET	PEN
6.2 ± 0.3°	4.9 ± 1.0°	6.8 ± 2.7°

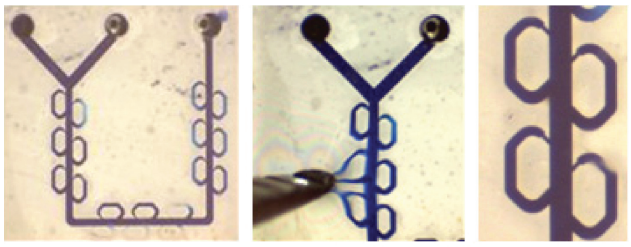

FIGURE 5 Optical microscope images of (a) toluidine blue injected into the device after prior injection of propanol, with (b) exerted pressure, and (c) removal of pressure with no exhibited leakage. An increase in pressure was applied for the PDMS–thermoplastic bonding.

and shows the strength of the APTES bonding was strong enough to support fluidic injection.

Application: Micromixing

Injection of Two Dyes

Prior injection of propanol on PI has improved the hydrophilicity. As Figure 6(a) shows the two dyes entered parallel to each other into the microchannel and then into the mixing loops in the form of a laminar flow regime (Y-shaped configurations). In Figure 6(b), the flow of the two dyes continued with the yellow (i) and blue (iv) dyes consistent in the mixing loops. However, within the microchannel, the two dyes do not run parallel as seen in Figure 6(a). Here, the yellow (ii) and blue (iii) dyes were seen merging. This demonstrates the beginning stages of mixing that was created by the mixing loops. The collision of the two liquids created by propulsion from the mixing loop exit is evident in (iv). The region around this exit is transparent and significant to iron(III) injection that has been forced back into the microchannel and across the flow path. Around the outer area, the color was darker. With increased time and injection at the same position on the microchannel, increased mixing can be seen [Fig. 6(c)]. The image has been contrast enhanced. Here, the two dyes are seen to run parallel to each other (i). On entering into the mixing loop (ii) the blue and yellow dyes have interacted and turned pale green. The green coloration lightens appearing green/yellow as it proceeds through the mixing loop (iii). With the fluidic flow of more iron(III), the previous pale green was forced along the microchannel wall (iv). At (v) the coloration at the mixing loop entrance was a darker shade of green as compared with (ii). This was also seen at (vi) in comparison to (iii). This demonstrates increased mixing and recirculation as the fluid encounters more mixing loops, thus becoming darker in color. With increased injection of iron(III), the green color formed within

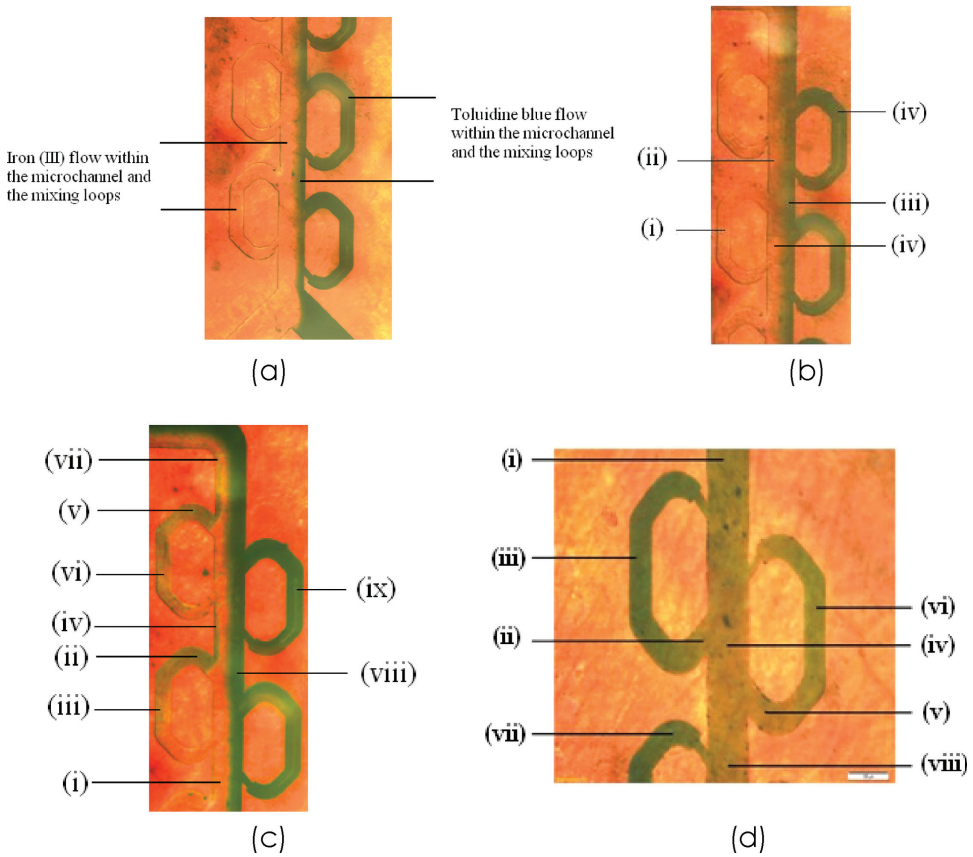

FIGURE 6 Micromixing by the injection of propanol followed by back aspiration of toluidine blue and iron(III) nitrate through a PDMS micromixer bonded to PI film. (a) Initial injection, (b) the start of mixing by chaotic advection, (c) increased injection of dyes, and (d) the start of the green-color saturation as a cause of mixing [5× objective taken for (a)–(c) and 10× for (d)].

the mixing loops was drawn along the microchannel wall in (iv) and (vii). A strong concentration of toluidine blue was still visualized in the microchannel (viii) and within the mixing loop (ix) as the two dyes flowed through the device.

Further along the microchannel, increased mixing has caused the two dyes to merge and now only a variation of the color green was seen [Fig. 6(d)]. Here, the dye in the microchannel was pale green (i). On entering into the mixing loop, the color seemed to have lightened (ii), though the concentration of the color has intensified to a darker green within the mixing loop (iii) due to the side of initial toluidine blue injection. After being forced back into the microchannel the dye was paler (iv) demonstrating increased mixing where it entered into the next mixing loop (v). The efficient mixing of the dyes can be seen clearly within this mixing loop. Because of the initial laminar flow of the iron(III) solution, the concentration of the dye was pale green illustrating that mixing has occurred. Upon entering this mixing loop the color intensified to a rich green color (vi), thus demonstrating that mixing has occurred from previous mixing loops and through the microchannel. An increase of the blue dye had diffused with more of the iron(III) solution within this mixing loop creating a vibrant green color. At (vii) the dyes were concentrated near the exit of the mixing loop, although this color was paler than that at the previous exit of the mixing loop (iii) and again demonstrates that the toluidine blue was mixing with the iron(III) solution. Returning to the microchannel (viii), a paler green color due to mixing was observed due to the evident mixing occurring as the dyes continued along the microchannel with increased fluidic flow.

In comparison of Figure 6(a–d), we visualize the laminar fluid flow of the two injected liquids entering into the microchannel within the first four mixing loops. Figure 6(d) (rotated 90°) showed the two inks had mixed between the next set of mixing loops. At this stage, we observed that the two dyes had mixed in comparison to Figure 6(a) with increased propulsion generated in Figure 6(b, c). On observation of the final six mixing loops, the liquids had comprehensively mixed and this displays that the passive micromixer containing 18 mixing loops and a microchannel length of 6.2 mm was capable of inducing total mixing by recirculation of the two injected dyes. The formation of a laminar and parallel fluidic flow at the beginning of the microchannel can indicate a parallel lamination micromixer. However, as both the PDMS micromixer and thermoplastic films are hydrophobic, this factor can contribute to the formation of the observed fluidic flow. Yet, this phenomenon was overcome at the end of the microchannel as completed mixing was observed. In this instance, if only diffusion was occurring, then no complete mixing would have been observed due to the short length of the applied microchannel.

To demonstrate mixing a magnified view of one of the loops was shown (Fig. 7). The image has been contrast enhanced and was taken at 10 × objective. A PDMS micromixer was bonded to PET film and the ink at (a) appeared pale yellow/green due to previous mixing. A pale yellow/green coloration

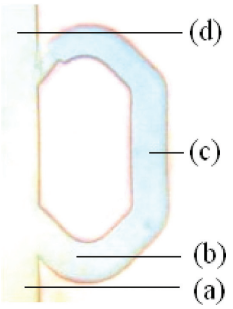

FIGURE 7 Injection of toluidine blue and iron(III) nitrate nonahydrate with a magnified view of the PDMS mixing loop based on PET film.

was seen entering into the mixing loop (b), whereby the coloration intensified (c) to pale blue due to the side of initial injection of toluidine blue. The mixed dyes were then forced back into the microchannel from the mixing loop exit that formed a pale green color (d) demonstrating mixing by this passive micromixer.

Injection of a Surfactant

As previously observed in Figure 6(b) (iv), the propulsion created by the mixing loops within the PDMS micromixer system has enabled mixing and recirculation of the liquids. In linear microchannels, mixing is difficult to obtain as only molecular diffusion is occurring. For passive micromixers, topology in the device is required in order for complete mixing to occur. For instance, chaotic advection can be achieved by the insertion of obstacle structures within the mixing channel. The arrangement of obstacles can alter the fluidic flow and the force of the liquids to mix and create transversal mass transport.[18] These have included zig-zag microchannels that can produce recirculation around the turns of the designed microchannel. For our designed micromixer in Figure 8, we demonstrate the injection of a surfactant with toluidine blue for the observation of how the mixing loops enable mixing to occur. In Figure 8(a), toluidine blue followed by the surfactant (with increased viscosity) was injected into the PDMS micromixer based on PEN. The microchannel appears placid and yellow in coloration due to the surfactant. In the two mixing loops, there appears to be a formation of large air globules as a cause of the beginning stages of mixing and chaotic advection between the two liquids. In Figure 8(b), the microchannel is not placid and yellow globules can be observed with a pale green coloration in its surroundings. This demonstrates an increase in velocity within the microchannel. The large globules within the mixing loops have now traveled further through the mixing loop. By Figure 8(c), an increased flow of toluidine blue was observed on the right wall of the microchannel and the microchannel was now full of globules. This demonstrates the interaction and mixing of the two liquids as a cause of increased velocity created by the mixing loops. By Figure 8(d), we see larger globules within the microchannel and smaller air globules in the mixing loops. At this stage, the velocity of the fluidic flow was decreasing. An increase of

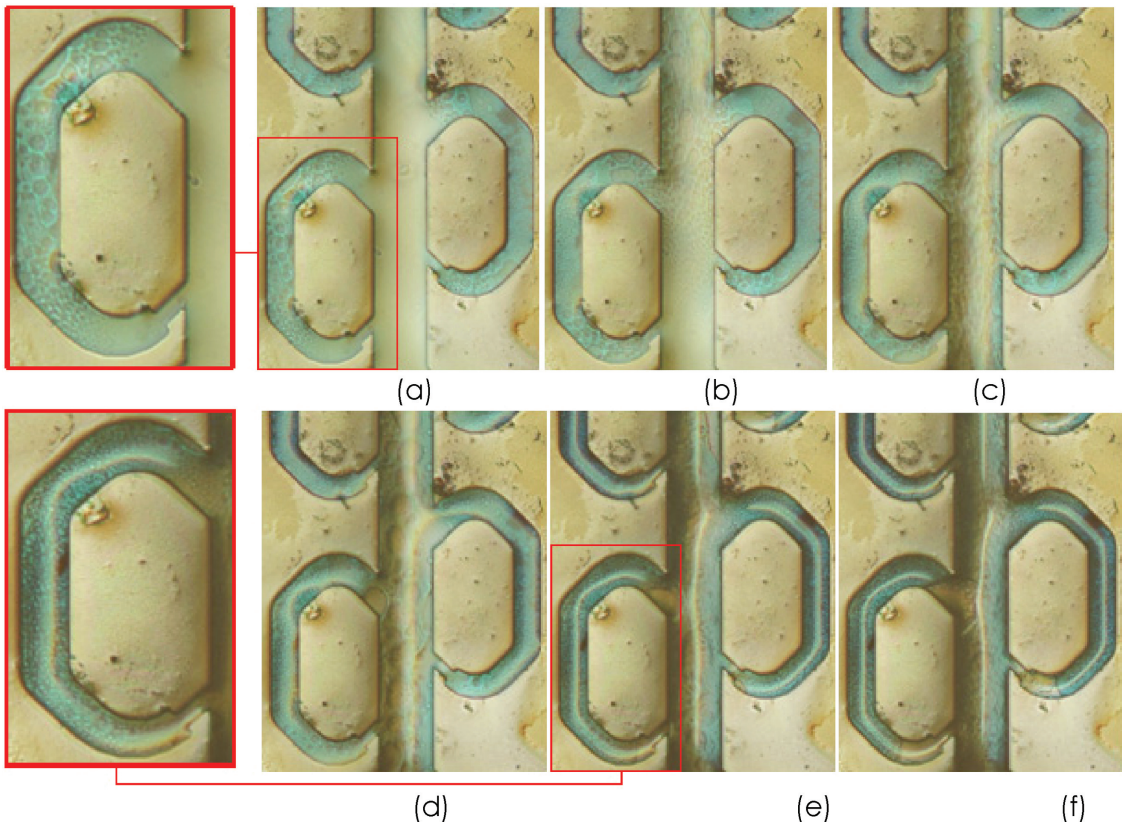

FIGURE 8 The injection of a surfactant with toluidine blue to formulate an increase in air bubbles/globules due to the propulsion created by the mixing loops (20×).

toluidine can be observed on the right side of the microchannel. The propulsion created the mixing loops is apparent within this image, due to the formation of yellow globules on the side of toluidine blue injection. In Y-shaped or T-shaped microchannels, the injection of two inks run parallel and mixing is a cause of molecular diffusion. Here, as the two fluids run parallel, the propulsion from the mixing loops has enabled the yellow globules to cross this intersection and chaotically mix with toluidine blue. Finally, by Figure 8(e,f), a parallel fluidic flow between the surfactant and toluidine blue was observed. Here, the fluidic flow has been further decreased. The mixing loops are still occupied by the smaller air globules as an effect of chaotic advection, while the coloration within the mixing loops has intensified with the increase of toluidine blue from Figure 8(a) to (f). This demonstrates increased mixing and the interaction of the surfactant with toluidine blue on opposing sides to the initial injection of the two liquids. Therefore, due to the geometry of the mixing loops, the interaction of the surfactant and toluidine blue was apparent. The larger globules transforming into smaller air bubbles demonstrate that mixing was occurring at velocity that was created by the mixing loops. Although we can observe parallel flow, the two liquids were capable of merging by the propulsion of the mixing loops (it must be noted that the viscosity of the surfactant was higher than that of toluidine blue). As there are no obstacles within the microchannel, chaotic advection and recirculation are created by designs that contain specific structures (e.g., obstacles on the wall,[34] obstacles in the channel,[35] and zig-zag shaped channel.[36] In our designed micromixer, these are attributable to the functionality of the 18 mixing loops.

Mixing Performance by pH Measurements

Applying a control, we can observe the color reading of pH 10 [Fig. 9(a)] and pH 2 [Fig. 9(b)]. By adding the same volume of pH 10 with pH 2, the liquids were mixed by vortex and the resulting solution formulated pH 7 by litmus test [Fig. 9(c)]. For the micromixer, the two varying pHs were injected into the Y-inlet simultaneously and the result was

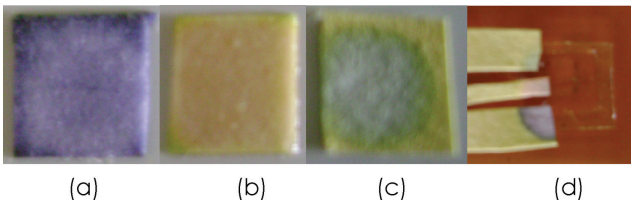

FIGURE 9 Mixing performance of the micromixer by analyzing the variation of pH to formulate a neutral pH, where, the control: (a) pH 10, (b) pH 2, (c) combination of pH 10 and pH 2, and (d) micromixer injection to demonstrate complete mixing.

observed by litmus test [Fig. 9(d)]. The resulting liquid at the exit port demonstrates the same pH as the control. Therefore, this confirms that the mixing performance of the passive micromixer containing 18 mixing loops and a short microchannel length of 6.2 mm was capable of inducing total mixing of the two injected pH solutions. This demonstrates the feasibility of the technology, applied with APTES bonding, followed by functional micromixers on hydrophobic polymers, which were capable of ultimately mixing two injected samples.

CONCLUSIONS

The fabrication of a micromixer based on polymers has been successfully demonstrated. A high total surface energy that was similar to glass was essential for PDMS–thermoplastic film bonding, and characterization by CAM, SFE, and XPS has shown that the thermoplastic films have been functionalized with APTES. With reduced dimensions and varying flow throughput in the form of passive micromixers, we produce to our knowledge the first reported PDMS–thermoplastic film bonding with micromixing of two different dyes, the propulsion of fluidic flow created by the mixing loops that formulate air through a surfactant, and by a pH test, we have demonstrated that the designed and fabricated micromixer is capable of complete mixing. The PDMS micromixers consisted of varying dimensions that did not disrupt the bonding process as several aspect ratios were under exerted pressure for adhesion. At first, the ink was unable to travel through the mixing loops, and we have demonstrated that this was not a factor of the given aspect ratios, but due to the hydrophobicity within the microchannel. By application of a solvent before use, we can alter the surface chemistry of the polymer film shortly to ensure that injected solutions can flow into all sections of the micromixer. The application of a micropump may assist on increasing the pressure gradient within the microchannel to create dispersion of the liquid within the mixing loops, or functionalization of the microchannel/mixing loops with polar structures may also aid this issue. These preliminary results demonstrate the feasibility of the fabrication technology, bonding technique, and application of the micromixer. Future experiments will analyze the bonding strength by load–displacement curves and analyze biological material for mixing before integration into a micro-total analysis system (μ-TAS).

ACKNOWLEDGEMENTS

The authors thank Francois Bessueille for his advice during the completion of this work. The authors acknowledge the funding through the Ministère de L'enseignement Supérieur et de la Recherche (MESR) and from the SensorART project, funded by the European Communities Seventh Framework Programme (FP7/2007-2013), under the grant agreement No. 248763, and by the Spanish Government through the MINAHE 3 project MEC-TEC2008-06883-CO3-01, and it reflects only the authors' views.

REFERENCES AND NOTES

1 Mills, C. A.; Martinez, E.; Bessueille, F.; Villanueva, G.; Bausells, J.; Samitier, J.; Errachid, A. *Microelectron. Eng.* **2005,** *78-79*, 695–700.

2 Mills, C. A.; Fernandez, J. G.; Errachid, A.; Samitier, J. J. *Microelectron. Eng.* **2008,** *85*, 1897–1901.

3 Rhee, S. W.; Taylor, A. M.; Tu, C. H.; Cribbs, D. H.; Cotman, C. W.; Jeon, N. L. *Lab. Chip* **2005,** *5*, 102–107.

4 Niskanen, A. J.; Ylinen-Hinkka, T.; Kulmala, S.; Frannssila, S. *Sens. Actuators B* **2011,** *152*, 56–62.

5 Xu, Y.; Lv, Y.; Wang, L.; Xing, W.; Cheng, J. *Biosens. Bioeletron.* **2012,** *32*, 300–304.

6 Bange, A.; Halsall, H. B.; Heineman, W. R. *Biosens. Bioeletron.* **2005,** *20*, 2488–2503.

7 Hu, B.; Siddiqui, J. A.; Ottenbrite, R. M. *Macromol. Chem. Phys.* **2002,** *203*, 1631–1635.

8 Wu, D.; Steckl, A. J. *Lab. Chip* **2009,** *9*, 1890–1896.

9 Tennico, Y. H.; Koesdjojo, M. T.; Kondo, S.; Mandrell, D. T.; Remcho, V. T. *Sens. Actuators B* **2010,** *143*, 799–804.

10 Becker, H.; Locascio, L. E. *Talanta* **2002,** *56*, 267–287.

11 Baraket, A.; Lee, M.; Zine, N.; Yaakoubi, N.; Trivella, M. G.; Zabala, M.; Bausells, J.; Jaffrezic- Renault, N.; Errachid, A. Cytokine detection using diazonium modified gold microelectrodes onto polyimide substrates with integrated Ag/AgCl reference electrode, Elsevier Procedia Engineering SI, Proc. Eurosensors 2012, September 9-12, **2012,** Krakow, Poland, DOI: 10.1016/j.proeng.2012.09.362.

12 Duffy, D. C.; McDonald, J. C.; Schueller, O. J. A.; Whitesides, G. M. *Anal. Chem.* **1998,** *70*, 4974–4984.

13 Bhusari, D.; Hayden, H.; Tanikella, R.; Allen, S. A. B.; Kohl, P. A. *J. Electrochem. Soc.* **2005,** *152*, 162–170.

14 Vlachopoulou, M.-E.; Tserepi, A.; Pavli, P.; Argitis, P.; Sanopoulou, M.; Misiakos, K. J. *Micromech. Microeng.* **2009,** *19*, 1–6.

15 Aran, K.; Sasso, L. A.; Kamdar, N.; Zahn, J. D. *Lab. Chip* **2010,** *10*, 548–552.

16 Tang, L.; Lee, N. Y. *Lab. Chip* **2010,** *10*, 1274–1280.

17 Sunkara, V.; Park, D.-K.; Hwang, H.; Chantiwas, R.; Soper, S. A.; Cho, Y.-K. *Lab. Chip* **2010,** *11*, 962–965.

18 Nguyen, N.-T.; Wu, Z. *J. Micromech. Microeng.* **2005,** *15*, R1–R16.

19 Hong, C.-C.; Choi, J.-W.; Ahn, C. H. *Lab. Chip* **2004,** *4*, 109–113.

20 Hossain, S.; Ansari, M. A.; Husain, A.; Kim, K.-Y. *Chem. Eng. J.* **2010,** *158*, 305–314.

21 Vijayendran, R. A.; Motsegood, K. M.; Beebe, D. J.; Leckband, D. E. *Langmuir* **2003,** *19*, 1824–1828.

22 Wong, S. H.; Ward, M. C. L.; Wharton, C. W. *Sens. Actuators B* **2004,** *100*, 359–379.

23 Kakuta, M.; Bessoth, F. G.; Manz, A. *TCR* **2001,** *1*, 395–405.

24 Capretto, L.; Cheng, W.; Hill, M.; Zhang, X. *Top. Curr. Chem.* **2011,** *304*, 27–68.

25 Hessel, V.; Lowe, H.; Schonfeld, F. *Chem. Eng. Sci.* **2005,** *60*, 2479–2501.

26 Lee, S.-H.; Kang, H.-J.; Choi, B. *Microsyst. Technol.* **2009,** *15*, 269–277.

27 Campbell, C. J.; Grzybowski, B. A. *Phil. Trans. R. Soc. Lond. A* **2004,** *362*, 1069–1086.

28 Lopez-Martinez, M. J.; Campo, E. M.; Caballero, D.; Fernandez, E.; Errachid, A.; Esteve, J.; Plaza, J. A. *J. Micromech. Microeng.* **2009,** DOI: 10.1088/0960-1317/19/10/105013.

29 Lopez-Martinez, M. J. MicroNanoTools for Life Sciences, PhD Thesis, Instituto de Microelectrónica de Barcelona, IMB-CNM (CSIC), Barcelona, October **2008.**

30 Abgrall, P.; Gue, A. M. *J. Micromech. Microeng.* **2007,** *17*, R15–R49.

31 Caballero, D.; Pla-Roca, M.; Bessueille, F.; Mills, C. A.; Samitier, J.; Errachid, A. *Anal. Lett.* **2006,** *39*, 1721–1734.

32 Cotte, S.; Baraket, A.; Bessueille, F.; Gout, S.; Yaakoubi, N.; Jaffrezic-Renault, N.; Leonard, D.; Errachid, A. Positive Microcontact Printing using Wet Palladium Deposition. Poster presented as part of the Biosensors 2010 World Congress, Glasgow, UK, 26–28 May, **2010.**

33 Xia, Y.; Whitesides, G. M. *Angew. Chem. Int. Ed.* **1998,** *37*, 550–575.

34 Wong, S. H.; Bryant, P.; Ward, M.; Wharton, C. *Sens. Actuators B* **2003,** *95*, 414–424.

35 Wang, H.; Lovenitti, P.; Harvey, E.; Masood, S. *J. Micromech. Microeng.* **2003,** *13*, 801–808.

36 Mengeaud, V.; Josserand, J.; Girault, H. H. *Anal. Chem.* **2002,** *74*, 4279–4286.